

Collective Radiative Interactions in the Discrete Truncated Wigner Approximation

Christopher D. Mink¹ and Michael Fleischhauer¹

¹ RPTU Kaiserslautern-Landau

* cmink@rptu.de

July 24, 2023

Abstract

Interfaces of light and matter serve as a platform for exciting many-body physics and photonic quantum technologies. Due to the recent experimental realization of atomic arrays at sub-wavelength spacings, collective interaction effects such as superradiance have regained substantial interest. Their analytical and numerical treatment is however quite challenging. Here we develop a semiclassical approach to this problem that allows to describe the coherent and dissipative many-body dynamics of interacting spins while taking into account lowest-order quantum fluctuations. For this purpose we extend the discrete truncated Wigner approximation, originally developed for unitarily coupled spins, to include collective, dissipative spin processes by means of truncated correspondence rules. This maps the dynamics of the atomic ensemble onto a set of semiclassical, numerically inexpensive stochastic differential equations. We benchmark our method with exact results for the case of Dicke decay, which shows excellent agreement. We then study superradiance in a spatially extended three-dimensional, coherently driven gas and study the dynamics of atomic arrays coupled to the quantized radiation field. For small arrays we compare to exact simulations, again showing good agreement at early times and at moderate to strong driving.

Contents

1	Introduction	2
2	Wigner Representation for Spins	3
2.1	Wigner representation of two-level systems	4
2.2	Time evolution of the Wigner function	4
2.3	An example for an exact FPE: spontaneous emission of a single two-level atom	6
2.4	The general case: Truncated Wigner Approximations (TWA) as diffusion approximations	6
3	Truncated Wigner Approximation for Large Spin Ensembles with Collective Couplings	7
3.1	Semiclassical limit of the correspondence rules for collective operators	7
3.2	Validity of the approximate correspondence rules	8
3.3	Two-body interactions and collective dephasing	10
4	TWA Description of Collective Light Emission	11
5	Dicke Decay	14

6	Dynamics of Spatially Extended Systems	16
6.1	Superradiance from an extended atomic cloud driven by an external laser	16
6.2	Driven atomic arrays	18
6.3	Inverted atomic arrays	18
7	Conclusion	19
	References	20

1 Introduction

The accurate description of non-equilibrium dynamics of interacting quantum spin systems is one of the major challenges of many-body theory. At the same time it is of central importance in many areas of physics. A prime example is the collective interaction of two-level atoms with the quantized electromagnetic field, which after integrating out the radiation field can be mapped onto collectively coupled spins with long-range interactions and dissipation. Collective light-matter interactions have been a central problem in quantum optics starting from the early work of Dicke [1]. Dicke showed that an ensemble of closely spaced two-level quantum emitters can display intriguing collective effects in the emission of light such as sub- and superradiance [2, 3] observed in a number of experiments [4–6]. This collective coupling between light and atoms has recently regained substantial interest as it is at the heart of many photonic quantum technologies [7]. Collective light-atom couplings are for example the basis of ensemble-based quantum memories for photons [8–10], quantum repeaters [11], and many concepts for realizing strongly interacting photons [12–15]. Here the interplay of the nonlinear atomic response and quantum entanglement results in rich coherent many-body dynamics.

A comprehensive theoretical treatment of the collective interaction of light with quantum emitters is however only simple if the spatial extension of the emitters can be neglected as in the case of the Dicke model or in cavity QED. Spatially extended systems can only be described by solving the Master equation, e.g. by Monte-Carlo Wave Function (MCWF) simulations [16], if the number of excitations is small or for small ensemble sizes. Numerical techniques based on Matrix Product States [17], which have proven to be extremely powerful for one-dimensional systems with short-range couplings are usually not appropriate in higher spatial dimensions and for long-range couplings. Likewise a classical treatment of collective phenomena in terms of Maxwell-Bloch equations neither captures the buildup of quantum correlations between the atoms. While some universal features of superradiance can be predicted for spatially extended systems without involved numerics [18, 19], there is for example no simple access to the timing and intensity of superradiant bursts. Expanding on the classical mean-field description in terms of Maxwell-Bloch equations, cumulant expansion techniques have been employed to account for correlations [20–22], but generally require higher order expansions for accurate predictions. Cumulant expansions are furthermore often ill-controlled and can suffer from intrinsic instabilities. Moreover their numerical complexity grows as a power law of the expansion order n , i.e. scales as N^n , where N is the number of spins, making them computationally expensive. The same holds for non-equilibrium Greens function approaches such as the one employed in [23].

In the present paper we propose an alternative, semiclassical approach that allows to describe the coherent and dissipative many-body dynamics of interacting spins, taking into ac-

count lowest-order quantum fluctuations. Our approach is inspired by the success of the discrete truncated Wigner approximation (DTWA) for the treatment of unitarily interacting spin systems [24], which has recently been extended to include single-particle dissipation [25–27]. Within the truncated Wigner approximation the dissipative many-body dynamics of spins is mapped to a generalized diffusion problem of the Wigner quasi-probability distribution in phase space. The exact relation between the dynamics of the many-body density matrix in Hilbert space and the Wigner function in phase space is given by correspondence rules, which lead to higher-order partial differential equations for the Wigner function. These are in general intractable without further approximations. A very successful approximation applicable to unitarily coupled spins is the DTWA, which can be extended to include single particle decay and dephasing [25]. The approach of Ref. [25] is however not useful for collective dissipative processes such as superradiance. We here pursue a different route. We propose approximate correspondence rules which lead to Fokker-Planck type equations of motion for the Wigner quasi distribution equivalent to a set of coupled stochastic differential equations (SDEs) for spin amplitudes. Since the number of these equations scales linearly in the number of spins, the solution is numerically inexpensive and allows investigating system sizes much larger than in other semiclassical approaches. In the truncated Wigner approximation quantum fluctuations are taken into account to lowest order by nondeterministic initial conditions and by collectively coupling the spins to white noise processes, which generate (weak) entanglement between the spins.

Our paper is organized as follows: In Sect. 2 we give a compact summary of the Wigner phase space representation of an ensemble of two-level systems (spins) using a continuous representation. We introduce a truncated Wigner Approximation for spin ensembles with collective couplings in Sect. 3. In particular we propose and motivate approximate correspondence rules and discuss general conditions for their validity. The main application of our methods are collective light-matter couplings in free space, which we will introduce in Sect. 4. In Sect. 5 we benchmark our method for the Dicke model, i.e. the collective emission of light from a tightly localized ensemble of two-level atoms, for which the full Master equation can be solved exactly. We find excellent agreement and give a physical interpretation of the emerging collective response within the semiclassical approximation. We then study collective light-matter phenomena in spatially extended systems in Sect. 6, where the full dynamics can no longer be described exactly. We consider superradiance from an elongated cloud of coherently driven atoms as well as regular arrays of atoms. Finally Sect. 7 summarizes the results and gives an outlook to future work.

2 Wigner Representation for Spins

An approach widely used in quantum optics to describe the dynamics of interacting, driven-dissipative many-body systems beyond the mean-field level is the truncated Wigner approximation (TWA) [28–32]. It describes interactions on a mean-field level but allows taking both thermal and leading-order quantum fluctuations into account by averaging over nondeterministic initial conditions and by coupling to stochastic noise sources. In the following we will give a compact summary of the Wigner representation of an ensemble of two-level systems or spins, but refer to Refs. [33, 34] for a more general introduction to phase-space representations in quantum mechanics. We formulate the TWA by studying the correspondence rules [35], which translate the action of an operator in Hilbert space to a differential operator in phase space, and show that they have a simple asymptotic limit for collective processes.

2.1 Wigner representation of two-level systems

The connection between Hilbert space and Wigner phase space, spanned by some c-number variables Ω is given by the representation of an operator \hat{O} in terms of a complex function $W_{\hat{O}}(\Omega)$, called the Weyl symbol

$$\hat{O} = \int d\Omega W_{\hat{O}}(\Omega) \hat{\Delta}(\Omega). \quad (1)$$

Here $\hat{\Delta}(\Omega)$ is the so-called phase point operator or Wigner kernel. Inversely the Weyl symbol can be expressed explicitly in terms of the operator by

$$W_{\hat{O}}(\Omega) = \text{Tr}[\hat{\Delta}(\Omega) \hat{O}]. \quad (2)$$

Of particular interest is the Weyl symbol $W_{\hat{\rho}}(\Omega)$ of the density operator $\hat{\rho}$, which is called the Wigner function or Wigner (quasi-probability) distribution. The latter notion is due to the fact that $W_{\hat{\rho}}(\Omega) \in \mathbb{R}$ and

$$\int d\Omega W_{\hat{\rho}}(\Omega) = \text{Tr}(\hat{\rho}) = 1, \quad (3)$$

but can be negative.

Originally formulated for continuous degrees of freedom the concept of phase space representations can be extended to systems with finite-dimensional Hilbert spaces [36] such as spin- $\frac{1}{2}$ systems. There is however some freedom in choosing the phase point operators. A specific discrete representation has been introduced by Wooters in [36], which is the basis of the discrete truncated Wigner approximation [24]. Here we adopt however a different, continuous representation of spin-1/2 states $\hat{\rho}$ through rotations of the particular discrete phase point operator $\hat{\Delta}_0 = \frac{1}{2}(\hat{1}_2 + \sqrt{3}\hat{\sigma}^z)$

$$\hat{\Delta}(\theta, \phi) = U(\theta, \phi, \psi) \hat{\Delta}_0 U^\dagger(\theta, \phi, \psi), \quad \Omega = (\theta, \phi) \quad (4)$$

which was shown in [25] to be more appropriate to describe dissipative spin systems. Here $U(\theta, \phi, \psi) = e^{-i\hat{\sigma}^z \phi/2} e^{-i\hat{\sigma}^y \theta/2} e^{-i\hat{\sigma}^z \psi/2}$, are the SU(2) rotation operators with Euler angles (θ, ϕ, ψ) , which gives

$$\hat{\Delta}(\theta, \phi) = \frac{1}{2}[\hat{1}_2 + \mathbf{s}(\theta, \phi) \hat{\boldsymbol{\sigma}}] = \frac{1}{2} \begin{pmatrix} 1 + \sqrt{3} \cos \theta & \sqrt{3} e^{-i\phi} \sin \theta \\ \sqrt{3} e^{i\phi} \sin \theta & 1 - \sqrt{3} \cos \theta \end{pmatrix}, \quad (5)$$

Note that in [25] we have used a slightly different definition of the Wigner kernel that is obtained by letting $\theta \rightarrow \pi - \theta$ and $\phi \rightarrow -\phi$.

We note furthermore that the vector $\mathbf{s}(\Omega)$ appearing in Eq. (5) is just the Weyl symbol of the Pauli spin-matrices

$$\mathbf{s}(\Omega) \equiv W_{\hat{\boldsymbol{\sigma}}}(\Omega) = \sqrt{3} \left(\sin \theta \cos \phi, \sin \theta \sin \phi, \cos \theta \right)^T. \quad (6)$$

The above can easily be extended to a system of N spin-1/2 systems via $\mathbf{s} \rightarrow \mathbf{s}_j$ and $\Omega \rightarrow \Omega = \{\Omega_j\}$, with $j = 1, 2, \dots, N$ labelling the spins.

2.2 Time evolution of the Wigner function

Our goal is to find an approximate solution of the master equation of many-body spin systems

$$\frac{d}{dt} \hat{\rho} = -i[\hat{H}, \hat{\rho}] + \frac{1}{2} \sum_{\mu} \left(2\hat{L}_{\mu} \hat{\rho} \hat{L}_{\mu}^{\dagger} - \{\hat{L}_{\mu}^{\dagger} \hat{L}_{\mu}, \hat{\rho}\} \right) \quad (7)$$

where the many-body Hamiltonian \hat{H} and the Lindblad operators \hat{L}_μ , describing Markovian dissipative processes, are some functions of the spin-1/2 operators $\hat{\sigma}_j^\mu$. Generically \hat{H} and/or the \hat{L}_μ describe interactions between spins which are higher dimensional, i.e. have couplings that cannot be reduced to a one-dimensional topology. The latter excludes in general effective descriptions in terms of matrix product states [17].

To develop an approximate, semiclassical approach we need to translate the master equation of the density operator $\hat{\rho}$ into an equation of motion for the Wigner function $W_\rho(\Omega)$. As the terms on the right hand side of Eq. (7) can be decomposed into products of spin operators and the density operator, this requires expressing the Weyl symbol of a composition of operators as emerging on the r.h.s. of (7), e.g. $\hat{H}\hat{\rho} \rightarrow W_{\hat{H}\hat{\rho}}$ in terms of the individual symbols $W_{\hat{H}}$ and $W_{\hat{\rho}}$. In phase space the Weyl symbol of a product does not correspond to a simple multiplication $W_{\hat{A}\hat{B}} \neq W_{\hat{A}} \cdot W_{\hat{B}}$ of the scalar functions. Instead, the composition is given by the *Moyal product* or *star product*

$$W_{\hat{A}\hat{B}}(\Omega) = W_{\hat{A}} \star W_{\hat{B}} = \iint d\Omega' d\Omega'' W_{\hat{A}}(\Omega') W_{\hat{B}}(\Omega'') \text{Tr}[\hat{\Delta}(\Omega) \hat{\Delta}(\Omega') \hat{\Delta}(\Omega'')], \quad (8)$$

which also has a differential form [33, 37]. The so called *correspondence rules* allow us to express the star product of Weyl symbols involving a spin operator, such as $W_{\hat{\sigma}_j^\mu} \star W_{\hat{A}}$, as differential operators acting on $W_{\hat{A}}$. With these rules we can iteratively translate compositions of operators as they appear in the master equation of $\hat{\rho}$ into a partial differential equation for the Wigner function W_ρ .

A more direct approach for deriving phase space equations that we have recently considered [25] is based on a simple observation: For a continuous phase space representation of a single spin, generated by the kernel given in Eq. (5), the matrices $\hat{\Delta}$, $\partial_\theta \hat{\Delta}$, $\partial_\phi \hat{\Delta}$ and $\partial_\phi^2 \hat{\Delta}$ span the Hilbert space. Hence any product of operators $\hat{O}\hat{\Delta}$ or $\hat{\Delta}\hat{O}$ can be expressed as a differential operator acting on $\hat{\Delta}$. Therefore, as can be seen from Eq. (1), the same operator acting on $\hat{\rho}$ can be converted into a differential operator acting on the Wigner function. However, the infinitesimal volume elements $d\Omega_n$ are not constant due to the curved phase space. It is therefore instructive to express the correspondence rules in terms of the contravariant coordinates $(x^1, x^2) = (\theta, \phi)$ of the phase space of a single spin and the metric tensor $g_{\mu\nu}$ which is given by

$$g = \frac{1}{2\pi} \begin{pmatrix} 1 & 0 \\ 0 & \sin^2 \theta \end{pmatrix}. \quad (9)$$

The derivatives acting on the Wigner function are then given by covariant derivatives

$$\nabla_{x_n} = \frac{1}{\sqrt{\det(g)}} \frac{\partial}{\partial x_n} \sqrt{\det(g)} = \csc \theta_n \frac{\partial}{\partial x_n} \sin \theta_n \quad (10)$$

with $x_n = \theta_n, \phi_n$. This yields correspondence rules such as [25]

$$\hat{\sigma}^z \hat{\rho} \leftrightarrow \left[\sqrt{3} \cos \theta + \nabla_\theta \frac{3 \sin \theta - 2 \csc \theta}{\sqrt{3}} - \nabla_\phi i + \nabla_\phi^2 \frac{2 \cot \theta \csc \theta}{\sqrt{3}} \right] W_\rho(\Omega). \quad (11)$$

A full list of these rules but in the aforementioned different angle convention is given in Ref. [25].

For general spin- j systems, exact expressions for the correspondence rules are known [35], but are complicated. They do have a simple semiclassical form in the limit $j \rightarrow \infty$, but for $j = 1/2$, which is by far the most commonly considered case in many branches of physics, this semiclassical limit is not directly applicable.

2.3 An example for an exact FPE: spontaneous emission of a single two-level atom

Let us start by applying the correspondence rules such as Eq. (11) to the important simple example of spontaneous decay, where an exact FPE can be derived. Two-level atoms in free space can undergo spontaneous relaxation to the energetically lower state by emission of light quanta. This is due to the fundamental coupling of the atoms to the quantized electromagnetic field. The description of this phenomenon can be drastically simplified by assuming that the field is in equilibrium (which is the vacuum at optical frequencies) and by subsequently integrating out the field's degrees of freedom. A Born-Markov approximation then yields the effective Lindblad master equation [38]

$$\frac{d}{dt}\hat{\rho} = \frac{\Gamma_0}{2}(2\hat{\sigma}^-\hat{\rho}\hat{\sigma}^+ - \hat{\sigma}^+\hat{\sigma}^-\hat{\rho} - \hat{\rho}\hat{\sigma}^+\hat{\sigma}^-) \quad (12)$$

for the density operator $\hat{\rho}(t)$ of an individual atom. The rate Γ_0 is the Einstein A coefficient.

As shown in [25] this master equation can be mapped onto a Fokker-Planck equation for the Wigner function $W_\rho(\Omega, t)$ without further approximations:

$$\begin{aligned} \frac{\partial}{\partial t}W_\rho(\Omega, t) = & -\Gamma_0\nabla_\theta\left(\cot\theta + \frac{\csc\theta}{\sqrt{3}}\right)W(\Omega, t) \\ & + \frac{\Gamma_0}{2}\nabla_\phi^2\left(1 + 2\cot^2\theta + \frac{2\cot\theta\csc\theta}{\sqrt{3}}\right)W_\rho(\Omega, t). \end{aligned} \quad (13)$$

It has an equivalent set of Itô SDEs [39, 40]

$$d\theta = \Gamma_0\left(\cot\theta + \frac{\csc\theta}{\sqrt{3}}\right)dt, \quad (14a)$$

$$d\phi = \sqrt{\Gamma_0\left(1 + 2\cot^2\theta + \frac{2\cot\theta\csc\theta}{\sqrt{3}}\right)}dW_\phi, \quad (14b)$$

where dW_ϕ is the differential of a Wiener process. These equations are exact and solving them is numerically inexpensive without further approximation.

2.4 The general case: Truncated Wigner Approximations (TWA) as diffusion approximations

Knowing the exact phase space formulation of the master equation shifts the quantum many-body problem of solving a large matrix differential equation of the density operator $\hat{\rho}(t)$, Eq. (7), to solving a high-dimensional partial differential equation with possibly infinitely many orders of derivatives for the c-number quasi-distribution $W_\rho(t)$. Except for special cases, such as the one discussed in Sec. 2.3, both formulations are useless without the introduction of further approximations.

From the perspective of complexity, the core idea behind different variants of the TWA consists of neglecting higher order terms of the equation of motion of $W_\rho(\Omega, t)$ such that the remaining expression is a covariant Fokker-Planck equation (FPE) in terms of suitable phase space variables Ω

$$\frac{\partial}{\partial t}W_\rho(\Omega, t) = -\sum_{x\in\Omega}\nabla_x A_x(\Omega, t)W_\rho(\Omega, t) + \frac{1}{2}\sum_{x,y\in\Omega}\nabla_x\nabla_y D_{xy}(\Omega, t)W_\rho(\Omega, t), \quad (15)$$

where $\mathbf{D}(\Omega, t) = \mathbf{B}(\Omega, t)\mathbf{B}^T(\Omega, t) \in \mathbb{R}^{2N \times 2N}$ is a positive semidefinite matrix. It then can be equivalently expressed by the set of SDEs [41]

$$d\mathbf{x} = \mathbf{A}(\Omega, t)d\mathbf{t} + \mathbf{B}(\Omega, t)d\mathbf{W}, \quad (16)$$

where $d\mathbf{W} \in \mathbb{R}^{2N}$ is a multivariate differential Wiener process. This and all further SDEs will implicitly be stated in the Itô calculus.

In a numerical implementation, we can efficiently compute N_{traj} independent solutions of the SDEs [42], which we call *trajectories*. All relevant expectation values can then be directly calculated in the Wigner phase by using the relation

$$\text{Tr}(\hat{\rho}\hat{O}) = \int d\Omega W_{\hat{\rho}}(\Omega)W_{\hat{O}}(\Omega) = \overline{W_{\hat{O}}(\Omega)}. \quad (17)$$

The bars indicate the stochastic average

$$\overline{W_{\hat{O}}(\Omega)} \approx \frac{1}{N_{\text{traj}}} \sum_{n=1}^{N_{\text{traj}}} W_{\hat{O}}(\Omega^{(n)}), \quad (18)$$

where $\Omega^{(n)}$ refers to the phase space coordinate of the n 'th trajectory and where the approximation due to a stochastic error vanishes as we let $N_{\text{traj}} \rightarrow \infty$.

In summary this means that the time evolution of the Wigner function in TWA is governed by a diffusion process on the surfaces of the spheres for each individual spins that represents the Wigner phase space. From a physical standpoint this truncation should be formulated in a systematic fashion which elucidates its validity in terms of a smallness parameter.

When adding spin-spin interactions, such as Ising-type couplings, the resulting equation for $W_{\hat{\rho}}(\Omega, t)$ is no longer of Fokker-Planck type and approximations are needed. A commonly used approximation is the discrete truncated Wigner approximation (DTWA) [24], which essentially amounts to a mean-field factorization of the Wigner function. This approach always produces deterministic equations and cannot account for the noise expected in dissipative systems.

As shown in [26, 43] independent dephasing of spins can be incorporated in the DTWA, but the description of decay requires some ad-hoc modelling [44], which is not justified in general. Therefore it is not surprising that the standard DTWA cannot be applied to collective decay processes such as superradiance. We recently developed an alternative approach, termed hybrid continuous-discrete truncated Wigner approximation (CDTWA), which describes the time evolution of the many-body density operator by a *continuous* representation of the multi-spin Wigner function but performs the averaging over the initial distribution in a discrete representation [25]. The CDTWA incorporates (uncorrelated) decay and dephasing of the spins in a consistent way, but does not generally reveal which correlated terms can be neglected or not (see Sec. IV. E of Ref. [25]).

3 Truncated Wigner Approximation for Large Spin Ensembles with Collective Couplings

Neither the standard DTWA nor the CDTWA mentioned in the previous section are suitable for describing problems of collective couplings among spins. We now present an alternative approach based on an approximate form of the correspondence rules for collective spin processes and derive conditions for their validity.

3.1 Semiclassical limit of the correspondence rules for collective operators

If an ensemble of two-level atoms is confined to a small volume comparable in size with the wavelength of the dipole transition between the two states, the coupling to the quantized electromagnetic field leads to a correlated emission of photons known as sub- and superradiance.

Collective processes in an ensemble of N spins can be described in terms of collective operators

$$\hat{\mathcal{S}}(\mathbf{J}) = \sum_{n=1}^N J_n \hat{\sigma}_n \quad (19)$$

where the "degree of cooperativity" is encoded in the distribution of weights $\mathbf{J} = (J_1, J_2, \dots) \in \mathbb{C}^N$. For $J_1 = J_2 = \dots = J$ the operator $\hat{\mathcal{S}}(\mathbf{J})$ describes the maximally cooperative case of an all-to-all coupling, relevant e.g. for modelling Dicke superradiance, see Sect. 4, while a distribution of the J_n 's peaked for some index $n = j$ corresponds to the low-cooperativity case. The action of $\hat{\mathcal{S}}(\mathbf{J})$ on the state $\hat{\rho}$ can be exactly expressed as a differential operator acting on the Wigner function $W_{\hat{\rho}}(\boldsymbol{\Omega})$ in the phase space, however this differential operator does not have a simple form [34, 35]. For the resulting equation of motion for the Wigner function to be of practical use, we propose instead truncated correspondence rules

$$W_{\hat{\mathcal{S}}(\mathbf{J})\hat{\rho}}(\boldsymbol{\Omega}) \approx \mathcal{S}(\mathbf{J})W_{\hat{\rho}}(\boldsymbol{\Omega}) = \sum_{n=1}^N J_n (\mathbf{s}_n + L_n) W_{\hat{\rho}}(\boldsymbol{\Omega}), \quad (20a)$$

$$\text{with } L_n = i\nabla_{\theta_n} \begin{pmatrix} +\sin\phi_n \\ -\cos\phi_n \\ 0 \end{pmatrix} + i\nabla_{\phi_n} \begin{pmatrix} \cot\theta_n \cos\phi_n \\ \cot\theta_n \sin\phi_n \\ -1 \end{pmatrix}, \quad (20b)$$

where $\mathbf{s}_n(\boldsymbol{\Omega})$ is given by Eq. (6) and L_n is the angular momentum differential operator expressed in terms of covariant derivatives. Similarly we find the action

$$W_{\hat{\rho}\hat{\mathcal{S}}(\mathbf{J})^\dagger}(\boldsymbol{\Omega}) = W_{[\hat{\mathcal{S}}(\mathbf{J})\hat{\rho}]^\dagger}(\boldsymbol{\Omega}) \approx [\mathcal{S}(\mathbf{J})W_{\hat{\rho}}(\boldsymbol{\Omega})]^* \quad (21)$$

for operators acting from the right-hand side. Note that the above contributions are the first and third term on the right-hand side of Eq. (11), whereas the remaining terms denote "quantum corrections" to this lowest order contribution. The intuition behind this truncation is simple: For a single spin- j , the same semiclassical limit can be obtained by letting $j \rightarrow \infty$. This reveals that classical and quantum contributions separate in the Wigner phase space.

We note that this approximation leads to a Fokker-Planck equation for $W_{\hat{\rho}}$ without higher-order derivatives if the master equation is at most bilinear in the collective operators. This allows for an efficient simulation in terms of SDEs. Eqs. (20) are the central element of our approach and form the basis of the simulations of collective decay phenomena discussed in Sects. 4 and 6.

3.2 Validity of the approximate correspondence rules

We now discuss the range of validity of the truncated correspondence rules, Eqs. (20). To this end we first note that the density operator $\hat{\rho}$ of a system of N spins has the general form

$$\hat{\rho} = \sum_{\boldsymbol{\mu}} \rho_{\boldsymbol{\mu}} \hat{\sigma}_1^{\mu_1} \dots \hat{\sigma}_N^{\mu_N}, \quad \text{with } \boldsymbol{\mu} = (\mu_1, \mu_2, \dots), \quad (22)$$

and $\mu_j = (0, x, y, z)$, with $\hat{\sigma}^0 = \hat{1}$ and $s^0 = 1$, from which we can immediately deduce

$$W_{\hat{\rho}}(\boldsymbol{\Omega}) = \sum_{\boldsymbol{\mu}} \rho_{\boldsymbol{\mu}} s_1^{\mu_1} \dots s_N^{\mu_N}. \quad (23)$$

Note that this expression, while being exact, is only of formal use as the sum contains an exponentially large number of terms. It does allow us, however, to explicitly calculate the exact Weyl symbol of operators such as $\hat{\mathcal{S}}^z(\mathbf{J})\hat{\rho}$ through direct evaluation of Eq. (2) via Eq. (23):

$$W_{\hat{\mathcal{S}}^z(\mathbf{J})\hat{\rho}}(\boldsymbol{\Omega}) = \text{Tr}[\hat{\Delta}(\boldsymbol{\Omega})\hat{\mathcal{S}}^z(\mathbf{J})\hat{\rho}] = \sum_{\boldsymbol{\mu}} \rho_{\boldsymbol{\mu}} \sum_n J_n \text{Tr}[\hat{\Delta}(\boldsymbol{\Omega})\hat{\sigma}_n^z \hat{\sigma}_1^{\mu_1} \dots \hat{\sigma}_N^{\mu_N}].$$

Applying the spin algebra of the Pauli matrices and evaluating the individual Weyl symbols yields

$$W_{\hat{S}^z(J)\hat{\rho}}(\Omega) = \sum_{\mu} \rho_{\mu} \sum_n s_1^{\mu_1} \dots J_n (\delta_{\mu_n,0} s_n^z + \delta_{\mu_n,z} + i \epsilon_{z,\mu_n,\nu_n} s_n^{\nu_n}) \dots s_N^{\mu_N}, \quad (24)$$

where ϵ_{ijk} is the Levi-Civita symbol. The truncation approximation in Eqs. (20) of the same Weyl symbol is obtained, on the other hand, by applying the z -component of Eq. (20a) to the Wigner function in Eq. (23), which yields:

$$S^z(J)W_{\hat{\rho}}(\Omega) = \sum_{\mu} \rho_{\mu} \sum_n s_1^{\mu_1} \dots J_n (s_n^z s_n^{\mu_n} + i \epsilon_{z,\mu_n,\nu_n} s_n^{\nu_n}) \dots s_N^{\mu_N}. \quad (25)$$

To determine the error of Eq. (25) made by the truncated correspondence rule we define its difference to Eq. (24)

$$\begin{aligned} \delta^z(\Omega) &\equiv W_{\hat{S}^z(J)\hat{\rho}}(\Omega) - S^z(J)W_{\hat{\rho}}(\Omega) \\ &= \sum_{\mu} \rho_{\mu} \sum_n s_1^{\mu_1} \dots J_n (\delta_{\mu_n,0} s_n^z + \delta_{\mu_n,z} - s_n^{\mu_n} s_n^z) \dots s_N^{\mu_N} \\ &= \sum_{\mu} \rho_{\mu} \sum_n s_1^{\mu_1} \dots J_n (1 - \delta_{\mu_n,0}) (\delta_{\mu_n,z} - s_n^{\mu_n} s_n^z) \dots s_N^{\mu_N}. \end{aligned}$$

In a similar way we can proceed with the x - and y -components $\hat{S}^x(J)\hat{\rho}$ and $\hat{S}^y(J)\hat{\rho}$. This gives the full difference vector

$$\delta(\Omega) \equiv (\delta^x, \delta^y, \delta^z)^T(\Omega) = \sum_{\mu} \rho_{\mu} \sum_n s_1^{\mu_1} \dots J_n (1 - \delta_{\mu_n,0}) (\mathbb{1} - \mathbf{s}_n \mathbf{s}_n^T)^{\mu_n} \dots s_N^{\mu_N},$$

where the superscript μ_n indicates the μ_n 'th row of the given matrix. Finally, the error can be quantified by the norm of the vector $\delta(\Omega)$

$$\begin{aligned} \|\delta(\Omega)\|^2 &= \int d\Omega (|\delta^x|^2 + |\delta^y|^2 + |\delta^z|^2) \\ &= \sum_{\mu,\nu} \rho_{\mu}^* \rho_{\nu} \sum_n \left(f_{nn}^{\mu\nu} + \sum_{m \neq n} f_{mn}^{\mu\nu} \right). \end{aligned}$$

We now evaluate the diagonal and non-diagonal parts separately. We find for the diagonal contribution:

$$\begin{aligned} f_{nn}^{\mu\nu} &= |J_n|^2 (1 - \delta_{\mu_n,0}) (1 - \delta_{\nu_n,0}) \cdot \\ &\quad \int d\Omega s_1^{\mu_1} s_1^{\nu_1} \dots \sum_{i=x,y,z} (\delta_{\mu_n,i} - s_n^{\mu_n} s_n^i) (\delta_{\nu_n,i} - s_n^{\nu_n} s_n^i) \dots s_N^{\mu_N} s_N^{\nu_N} \\ &= 2^{N+1} (1 - \delta_{\mu_n,0}) \delta_{\mu,\nu} |J_n|^2, \end{aligned}$$

which follows from $\int d\Omega s_n^{\mu_n} s_n^{\nu_n} = \text{Tr}(\hat{\sigma}_n^{\mu_n} \hat{\sigma}_n^{\nu_n}) = 2\delta_{\mu_n,\nu_n}$ and $|\mathbf{s}_n|^2 = 3$. The off-diagonal components all vanish

$$f_{mn}^{\mu\nu} = 0, \quad \text{for } m \neq n,$$

as each contains factors

$$\int d\Omega s_n^{\mu_n} (1 - \delta_{\nu_n,0}) (\delta_{\nu_n,i} - s_n^{\nu_n} s_n^i) = 0.$$

Since

$$\mathrm{Tr}(\hat{\rho}^2) = \sum_{\mu, \nu} \rho_{\mu}^* \rho_{\nu} \mathrm{Tr}(\hat{\sigma}_1^{\mu_1} \hat{\sigma}_1^{\nu_1}) \dots \mathrm{Tr}(\hat{\sigma}_N^{\mu_N} \hat{\sigma}_N^{\nu_N}) = 2^N \sum_{\mu} |\rho_{\mu}|^2, \quad (26)$$

we see that

$$\begin{aligned} \|\delta(\Omega)\|^2 &= 2^N \sum_{\mu} |\rho_{\mu}|^2 \sum_{n=1}^N 2|J_n|^2 (1 - \delta_{\mu_n, 0}) \\ &\leq 2|J|^2 \mathrm{Tr}(\hat{\rho}^2). \end{aligned} \quad (27)$$

When $\hat{\rho}$ is the completely mixed state, we have $\mu_n = 0$ for every n and therefore the truncated correspondence rules are exact. For general states we can infer the error to scale as

$$\|\delta(\Omega)\| \sim |J| = \left[\sum_{n=1}^N |J_n|^2 \right]^{1/2}. \quad (28)$$

One recognizes that if the coefficients J_n all have comparable magnitudes we have

$$\|\delta(\Omega)\| \sim \mathcal{O}(\sqrt{N}). \quad (29)$$

A necessary condition for the asymptotic correspondence rules to be valid is that the relative deviation to the exact Weyl symbol is small, i.e.

$$\frac{\|\delta(\Omega)\|}{\|W_{\hat{S}(J)\hat{\rho}}\|} \ll 1. \quad (30)$$

Note that

$$\|W_{\hat{S}(J)\hat{\rho}}\| = \sqrt{\mathrm{Tr}(\hat{\rho}^2 \hat{S}^{\dagger}(J) \hat{S}(J))}. \quad (31)$$

This expression can maximally scale as $\mathcal{O}(N)$, in which case the truncation approximation Eq. (30) is satisfied for large ensemble sizes N . We now argue that this is the case if the dynamics of the system takes place in the subspace of states with large cooperativity. To this end consider the totally symmetric operators with $J_n \equiv 1$. The total angular momentum operator $\hat{S}^2 = \hat{S}(J)^{\dagger} \hat{S}(J)$ has eigenstates $|j, m, \alpha\rangle$ with so-called cooperativity $0 \leq j \leq \frac{N}{2}$, projection $|m| \leq j$ on the z -axis and the parameter α distinguishing degenerate states. If $\hat{\rho} = |j, m, \alpha\rangle\langle j, m, \alpha|$ and $j \neq 0$, then Eq. (30) yields

$$\frac{\|\delta(\Omega)\|}{\|W_{\hat{S}(J)\hat{\rho}}\|} \leq \frac{\sqrt{2N \langle j, m, \alpha | j, m, \alpha \rangle}}{|\langle j, m, \alpha | \hat{S}^2 | j, m, \alpha \rangle|^{1/2}} = \frac{\sqrt{2N}}{j} = \mathcal{O}\left(\frac{1}{\sqrt{N}}\right), \quad (32)$$

i.e. the cooperativity of the spin ensemble determines the validity of the asymptotic form of the correspondence rules.

3.3 Two-body interactions and collective dephasing

Before turning to specific applications of our TWA approach, let us discuss two special cases of collective spin-spin interactions and collective dissipative processes which are relevant e.g. for ensembles of two-level atoms coupled via a cavity field.

To describe the time evolution under the action of a collective interaction we can use the truncated correspondence rules of Eq. (20) resulting in

$$-\frac{i}{2}[\hat{S}^x(J)\hat{S}^x(J), \hat{\rho}] \xrightarrow{\approx} \sum_{mn} J_m J_n \left(+ \nabla_{\theta_m} \sin \phi_m s_n^x + \nabla_{\phi_m} \cot \theta_m \cos \phi_m s_n^x \right. \\ \left. + \nabla_{\theta_n} \sin \phi_n s_m^x + \nabla_{\phi_n} \cot \theta_n \cos \phi_n s_m^x \right) W_{\hat{\rho}}(\Omega), \quad (33a)$$

$$-\frac{i}{2}[\hat{S}^y(J)\hat{S}^y(J), \hat{\rho}] \xrightarrow{\approx} \sum_{mn} J_m J_n \left(- \nabla_{\theta_m} \cos \phi_m s_n^y + \nabla_{\phi_m} \cot \theta_m \sin \phi_m s_n^y \right. \\ \left. - \nabla_{\theta_n} \cos \phi_n s_m^y + \nabla_{\phi_n} \cot \theta_n \sin \phi_n s_m^y \right) W_{\hat{\rho}}(\Omega), \quad (33b)$$

$$-\frac{i}{2}[\hat{S}^z(J)\hat{S}^z(J), \hat{\rho}] \xrightarrow{\approx} \sum_{mn} J_m J_n \left(- \nabla_{\phi_m} s_n^z - \nabla_{\phi_n} s_m^z \right) W_{\hat{\rho}}(\Omega). \quad (33c)$$

The equivalent stochastic differential equations in θ_n, ϕ_n are in fact deterministic and quantum fluctuations enter only through the averaging over the Wigner distribution of the initial state. A change of variables $\theta_n, \phi_n \rightarrow \mathbf{s}_n$ to Cartesian coordinates then gives equations of the type

$$d\mathbf{s}_n = 2J_n \mathbf{S}^\mu(J) \times \mathbf{s}_n dt, \quad (34)$$

where $\mathbf{S}^\mu(J) = \sum_m J_m s_m^\mu \mathbf{e}_\mu$ with $\mu = x, y, z$. This is a Larmor precession of the vectors \mathbf{s}_n about the cumulative magnetic field $2J_n \mathbf{S}^\mu(J)$ and is equivalently predicted by a mean-field approximation and the standard DTWA.

In addition to unitary interactions described by a von Neumann equation, collective dissipative processes described by Linblad master equations are oftentimes of interest as well. A particularly simple case is that of *collective dephasing* for which we find an exact mapping to a FPE [34]

$$\frac{\gamma}{2} [2\hat{S}^z(J)\hat{\rho}\hat{S}^z(J) - \hat{S}^z(J)\hat{S}^z(J)\hat{\rho} - \hat{\rho}\hat{S}^z(J)\hat{S}^z(J)] \leftrightarrow \frac{\gamma}{2} \sum_{mn} \nabla_{\phi_m} \nabla_{\phi_n} 4J_m J_n W_{\hat{\rho}}(\Omega). \quad (35)$$

This equation has the equivalent set of very simple SDEs

$$d\theta_n = 0, \quad d\phi_n = 2\sqrt{\gamma} J_n dW. \quad (36a)$$

It is not surprising that all angles ϕ_n couple to the same noise dW , as their time evolution can equally be generated by a Hamiltonian contribution $\hat{H} = \gamma \hat{S}^z(J) \eta(t)$ where $\eta(t)$ is a white noise process with the identical properties as dW .

4 TWA Description of Collective Light Emission

Let us consider N two-level atoms with arbitrary but non-overlapping positions \mathbf{r}_n coupled to the quantized electromagnetic field at distances comparable to the wavelength λ_e of the two-level dipole transition. In contrast to the case of atoms spaced at distances much larger than λ_e , which allows a formal elimination of the coupling to the radiation field for each atom individually, leading to the effective Lindblad master equation (12), here radiative couplings between the atoms need to be taken into account. In addition we allow for a driving of the atoms by an external coherent light field

$$\mathcal{E}(\mathbf{r}, t) = e_c \mathcal{E}(\mathbf{r}) e^{-i\omega_c t} + \text{c.c.} \quad (37)$$

which is polarized along the unit vector \mathbf{e}_c and has the wave vector $\mathbf{k}_c = \mathbf{e}_n \omega_c / c$ with $\mathbf{e}_n \cdot \mathbf{e}_c = 0$. The corresponding Rabi frequency for the j 'th atom is $\Omega_j = \mathbf{p} \cdot \mathbf{e}_c \mathcal{E}(\mathbf{r}_j)$, where \mathbf{p} is the atomic transition dipole moment, which is assumed to be identical for all atoms. We denote the detuning between the classical field and the atoms as $\Delta = \omega_c - \omega_e$. Formally integrating out the electromagnetic field and using a Born-Markov approximation results in a master equation of the N atom system which reads [45]

$$\frac{d}{dt} \hat{\rho} = -i[\hat{H}, \hat{\rho}] + \frac{1}{2} \sum_{mn} \Gamma_{mn} (2\hat{\sigma}_m^- \hat{\rho} \hat{\sigma}_n^+ - \hat{\sigma}_m^+ \hat{\sigma}_n^- \hat{\rho} - \hat{\rho} \hat{\sigma}_m^+ \hat{\sigma}_n^-). \quad (38)$$

The effective Hamiltonian

$$\hat{H} = -\frac{\Delta}{2} \sum_n \hat{\sigma}_n^z - \sum_n (\Omega_n \hat{\sigma}_n^+ + \text{h.a.}) + \sum_n \sum_{m \neq n} J_{mn} \hat{\sigma}_m^+ \hat{\sigma}_n^-, \quad (39)$$

describes the coupling to the external coherent drive as well as the radiative coupling between the two-level atoms with rates J_{mn} . These rates as well as the positive definite decay matrix $\Gamma = \mathbf{G}\mathbf{G}^T \in \mathbb{R}^{N \times N}$, where the choice of \mathbf{G} is unique up to a unitary rotation which does not influence the dynamics, are given by the free space Green's tensor $\mathbf{G}_E(\mathbf{r}_m, \mathbf{r}_n, \omega_e)$ of the electric field

$$-J_{mn} + \frac{i}{2} \Gamma_{mn} = \frac{1}{\epsilon_0} \left(\frac{2\pi\omega_e}{c} \right)^2 \mathbf{p}^\dagger \cdot \mathbf{G}_E(\mathbf{r}_m, \mathbf{r}_n, \omega_e) \cdot \mathbf{p}. \quad (40)$$

Their explicit expressions are

$$\begin{aligned} \frac{J_{mn}}{\Gamma_0} = & -\frac{3}{4} \left\{ (1 - |\mathbf{e}_p \cdot \mathbf{e}_{r_{mn}}|^2) \frac{\cos(k_e r_{mn})}{k_e r_{mn}} \right. \\ & \left. - (1 - 3|\mathbf{e}_p \cdot \mathbf{e}_{r_{mn}}|^2) \left[\frac{\sin(k_e r_{mn})}{(k_e r_{mn})^2} + \frac{\cos(k_e r_{mn})}{(k_e r_{mn})^3} \right] \right\}, \end{aligned} \quad (41a)$$

$$\begin{aligned} \frac{\Gamma_{mn}}{\Gamma_0} = & \frac{3}{2} \left\{ (1 - |\mathbf{e}_p \cdot \mathbf{e}_{r_{mn}}|^2) \frac{\sin(k_e r_{mn})}{k_e r_{mn}} \right. \\ & \left. + (1 - 3|\mathbf{e}_p \cdot \mathbf{e}_{r_{mn}}|^2) \left[\frac{\cos(k_e r_{mn})}{(k_e r_{mn})^2} - \frac{\sin(k_e r_{mn})}{(k_e r_{mn})^3} \right] \right\}, \end{aligned} \quad (41b)$$

where $\mathbf{r}_{mn} = \mathbf{r}_m - \mathbf{r}_n$ and \mathbf{e}_p ($\mathbf{e}_{r_{mn}}$) is the unit vector along the polarization \mathbf{p} (the position \mathbf{r}_{mn}) and $k_e = c/\omega_e$. The diagonal elements $\Gamma_{nn} = \Gamma_0$ are given by the Einstein A coefficient and we set $J_{nn} = 0$, thereby absorbing it into the atomic detuning Δ . This contribution corresponds to the Lamb shift, which is however not correctly described within the dipole approximation of the atom-light coupling. In fact J_{nn} diverges since $r_{mn} \rightarrow 0$ for $m = n$. In the following sections we will assume resonant driving of the atoms and therefore set $\Delta = 0$.

An exact mapping of the master equation to phase space would go beyond a Fokker-Planck description, however the asymptotic correspondence rules of Eqs. (20) reduce it to

$$\frac{\partial}{\partial t} W_\rho(\boldsymbol{\Omega}, t) = \left(-\mathcal{L}_1 + \frac{1}{2} \mathcal{L}_2 \right) W_\rho(\boldsymbol{\Omega}, t), \quad (42a)$$

$$\begin{aligned} \mathcal{L}_1 = & \sum_{n=1}^N \left\{ \nabla_{\theta_n} \left[\frac{\Gamma_{nn}}{2} \cot \theta_n + \sqrt{3} \sum_{m=1}^N \sin \theta_m \left(J_{mn} \sin \phi_{mn} + \frac{\Gamma_{mn}}{2} \cos \phi_{mn} \right) \right] \right. \\ & \left. + \nabla_{\phi_n} \sqrt{3} \cot \theta_n \sum_{m=1}^N \sin \theta_m \left(-J_{mn} \cos \phi_{mn} + \frac{\Gamma_{mn}}{2} \sin \phi_{mn} \right) \right\}, \end{aligned} \quad (42b)$$

$$\begin{aligned} \mathcal{L}_2 = & \sum_{m,n=1}^N \Gamma_{mn} \left(\nabla_{\theta_m} \nabla_{\theta_n} \cos \phi_{mn} + \nabla_{\phi_m} \nabla_{\phi_n} \cot \theta_m \cot \theta_n \cos \phi_{mn} \right. \\ & \left. - \nabla_{\theta_m} \nabla_{\phi_n} \cot \theta_n \sin \phi_{mn} + \nabla_{\phi_m} \nabla_{\theta_n} \cot \theta_m \sin \phi_{mn} \right), \end{aligned} \quad (42c)$$

where $\phi_{mn} = \phi_m - \phi_n$. The equivalent set of SDEs is given by

$$d\theta_n = \left[\frac{\Gamma_{nn}}{2} \cot \theta_n + \sqrt{3} \sum_{m=1}^N \sin \theta_m \left(J_{mn} \sin \phi_{mn} + \frac{\Gamma_{mn}}{2} \cos \phi_{mn} \right) \right] dt + \sum_{m=1}^N G_{nm} (-\cos \phi_n dW_{\theta_m} + \sin \phi_n dW_{\phi_m}), \quad (43a)$$

$$d\phi_n = \sqrt{3} \cot \theta_n \sum_{m=1}^N \sin \theta_m \left(-J_{mn} \cos \phi_{mn} + \frac{\Gamma_{mn}}{2} \sin \phi_{mn} \right) dt + \sum_{m=1}^N G_{nm} \cot \theta_n (\sin \phi_n dW_{\theta_m} + \cos \phi_n dW_{\phi_m}), \quad (43b)$$

with $2N$ independent Wiener increments.

The single-particle terms can be treated exactly and yield

$$\frac{i\Delta}{2} [\hat{\sigma}_n^z, \hat{\rho}] \leftrightarrow \Delta \cdot \nabla_{\phi_n} W_{\hat{\rho}}(\Omega), \quad (44a)$$

$$\frac{i}{2} [\Omega_n \hat{\sigma}_n^+ + \Omega_n^* \hat{\sigma}_n^-, \hat{\rho}] \leftrightarrow - \left[\nabla_{\theta_n} \text{Im}(\Omega_n e^{i\phi_n}) + \nabla_{\phi_n} \text{Re}(\Omega_n e^{i\phi_n}) \cot \theta_n \right] W_{\hat{\rho}}(\Omega), \quad (44b)$$

which gives the following additional deterministic contributions

$$d\theta_n = \text{Im}(\Omega_n e^{i\phi_n}) dt, \quad (45a)$$

$$d\phi_n = [\text{Re}(\Omega_n e^{i\phi_n}) \cot \theta_n - \Delta] dt, \quad (45b)$$

to the above SDEs.

In the following sections we will investigate specific examples of atomic matter coupled to quantized light fields and demonstrate the strengths and weaknesses of the TWA by comparing its predictions of several observables to numerically exact results. An experimentally available observable is for example the total photon emission rate

$$\gamma(t) = \frac{d}{dt} \langle \hat{S}^z \rangle_{\Gamma} = \frac{1}{2} \sum_{m,n=1}^N \Gamma_{mn} \langle 2\hat{\sigma}_m^+ \hat{S}^z \hat{\sigma}_n^- - \hat{\sigma}_m^+ \hat{\sigma}_n^- \hat{S}^z - \hat{S}^z \hat{\sigma}_m^+ \hat{\sigma}_n^- \rangle \quad (46)$$

into all directions. We compute it directly from ensemble averages in phase space by applying Itô's lemma to the corresponding Weyl symbol $W_{\hat{S}^z} = \sqrt{3} \sum_n \cos \theta_n / 2$ in conjunction with Eqs. (43), hence obtaining

$$\gamma(t) = -\frac{\sqrt{3}}{2} \sum_n \Gamma_{nn} \overline{\cos \theta_n} - \frac{3}{4} \sum_{mn} \overline{\Gamma_{mn} \sin \theta_m \sin \theta_n \cos(\phi_m - \phi_n)}. \quad (47)$$

It is typically easier to detect the intensity of the emitted light into a solid angle with direction defined by the unit vector \mathbf{e}_k or small areas obtained from an integration over some geometric configuration thereof. The photon emission rate along the unit vector \mathbf{e}_k is proportional to [45]

$$\gamma(\mathbf{e}_k, t) = \gamma_0(\mathbf{e}_k) \sum_{m,n=1}^N e^{\frac{2\pi i}{\lambda_e} \mathbf{e}_k \cdot (\mathbf{r}_m - \mathbf{r}_n)} \langle \hat{\sigma}_m^+ \hat{\sigma}_n^- \rangle, \quad (48a)$$

$$\gamma_0(\mathbf{e}_k) = 1 - |\mathbf{e}_p \cdot \mathbf{e}_k|^2, \quad (48b)$$

where $\gamma_0(\mathbf{e}_k)$ is the enveloping emission profile of a single atom.

Moreover we consider the spin squeezing parameter ξ^2 defined as

$$\xi^2 = \frac{N}{|\langle \hat{\mathbf{S}} \rangle|^2} \min_{\mathbf{e}_n} (\Delta \hat{S}_{\mathbf{e}_n})^2, \quad (49)$$

where $\hat{\mathbf{S}} = (\hat{S}^x, \hat{S}^y, \hat{S}^z)^T$ is the collective spin operator and $\Delta \hat{S}_{\mathbf{e}_n} = \langle \hat{S}_{\mathbf{e}_n}^2 \rangle - \langle \hat{S}_{\mathbf{e}_n} \rangle^2$ is the variance of the operator $\hat{S}_{\mathbf{e}_n} = \mathbf{e}_n \cdot \hat{\mathbf{S}}$ projected onto an axis that is orthogonal to the mean spin, i.e. $\langle \hat{\mathbf{S}} \rangle \cdot \mathbf{e}_n = 0$. This minimal variance is not only of interest in quantum metrology, but furthermore a squeezing of $\xi^2 < 1$ implies entanglement [46].

5 Dicke Decay

To benchmark our method and to illustrate its strengths, we will first study the case where all atoms couple with identical rates $\Gamma_{mn} = \Gamma_0$, and where the unitary couplings are ignored $J_{mn} \equiv 0$. This model was proposed by Dicke as an approximation to the radiative coupling of a free gas at very strong confinement [1]. The model also typically arises as a contribution in cavity- and waveguide QED.

Substituting the resulting the most simple choice $G_{mn} = \sqrt{\Gamma_0} \delta_{n,1}$ such that $\mathbf{\Gamma} = \mathbf{G}\mathbf{G}^T$ into Eqs. (43) reveals that the phase space angles only couple to 2 of the possible $2N$ white noise processes. If the system is initially in the inverted state $|e_1 e_2 \dots e_N\rangle = |j = N/2, m = N/2\rangle$, it can only decay along the states of maximal cooperativity $j = N/2$. Hence we expect the TWA be a good approximation at large N . The ensemble descends this ladder of states with initially increasing and then decreasing rates. This gives rise to the effect of superradiance, i.e. the emission of light at a rate faster than that of a single atom [1]. Furthermore the restriction to just $N+1$ states means that an exact and efficient numerical integration of the master equation in terms of rates is possible [3].

In Fig. 1 we compare the TWA prediction of the number of excitations and the total emission rate to exact results. The TWA results were produced using an Euler-Maruyama integration scheme [42] with a timestep $\ln(N)\Gamma_0\Delta t/N = 10^{-3}$ and an averaging over $64 \cdot 10^3$ trajectories. They accurately reproduce the exact results. Even at small ensemble sizes of $N = 8$ a maximum absolute error of only $\approx 1\%$ occurs which further decreases in N . The positions and heights of the superradiant bursts are matched with similar accuracy.

Since only the states of maximal $j = N/2$ couple to the vacuum state $|g_1 g_2 \dots g_N\rangle$, other initial states cannot fully emit their excitations. This gives rise to the effect of *excitation trapping*. For simplicity consider even N . If we assume the initial state to be the completely mixed state, given by the factorized Wigner function $W_{\hat{\rho}}(\mathbf{\Omega}) = \prod_{n=1}^N W_{\hat{\rho}}^{(n)}(\Omega_n)$ with $W_{\hat{\rho}}^{(n)}(\Omega_n) = 1/2$, the steady state population can be determined by summing over the $(2j+1)d_j$ states in each j -ladder with degeneracy d_j and with probability 2^{-N} each and multiplying by the population $-j$ of the bottom state, leading to

$$\langle \hat{S}^z(t \rightarrow \infty) \rangle = \sum_{j=0}^{N/2} \frac{(2j+1)d_j}{2^N} (-j), \quad (50a)$$

$$d_j = (2j+1) \frac{N!}{(N/2+j+1)!(N/2-j)!}. \quad (50b)$$

In Fig. 1 d) and e) we again see a very good agreement of the TWA with the exact results that improves as N increases. We note that while the steady-state populations can be calculated exactly, the dynamics at arbitrary ensemble sizes starting from a mixed state cannot.

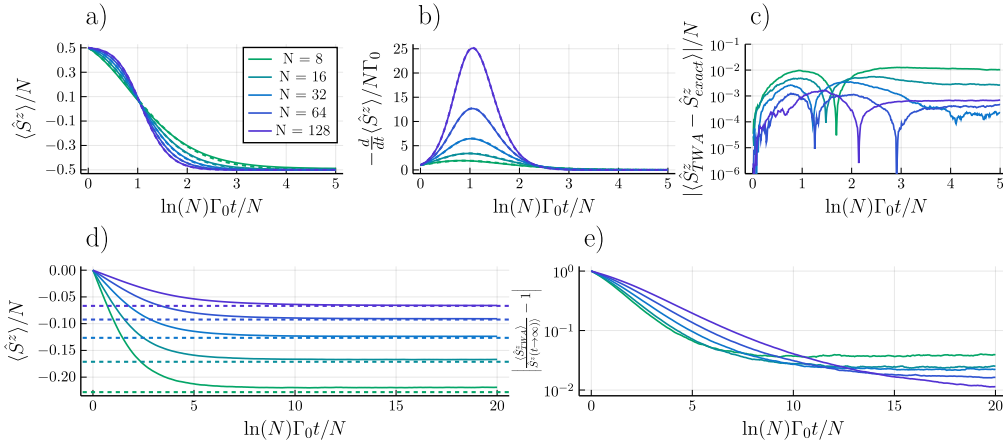


Figure 1: Dynamics of the Dicke decay for varying ensemble sizes N . For an initially inverted system the a) number of excitations and b) emission rate of are shown as predicted by the TWA (solid lines) and exact results (dashed lines). c) Absolute difference of the exact excitation number and TWA prediction. For the initially fully mixed state d) depicts population trapping of the excitation number. The dashed lines indicate the exact steady state populations. e) Time evolution of the relative deviation of the TWA population prediction from the exact steady state.

Furthermore, the Dicke decay is a prime example for revealing how superradiance emerges within our semiclassical approximation. With the assumption that $J_{mn} = 0$ and $\Gamma_{mn} = \Gamma_0$ we can see that the SDEs of Eqs. (43) are closely related to the Kuramoto model [47]

$$\frac{d}{dt} \phi_n = \omega_n + \sum_{m=1}^N K_{mn} \sin(\phi_m - \phi_n), \quad (51)$$

which describes harmonic oscillators with frequencies ω_n and pairwise coupling rates K_{mn} . If we compare this to the equations of the relative phases ϕ_n of the two-level states, we can identify $\omega_n = -\Delta = 0$ and $K_{mn} = \frac{1}{2}\Gamma_0 \sin \theta_m \cot \theta_n$. The coupling is long-ranged and, due to the appearing θ_m terms, time-dependent. Additionally, the phases are subjected to non-diagonal and non-linear noise. Nevertheless the origin of superradiant bursts in the Dicke model can be related to the phase transition in the Kuramoto model from a completely incoherent state where all $\{\phi_n\}$ are uniformly distributed to that of spontaneous synchronization. This emergence of synchronization $\phi_m = \phi_n$ causes a dynamic shift of the changes $d\theta_n$ and therefore of the total number of excitation $\langle \hat{S}^z \rangle$. As a result, the photon emission rate will transition from individually radiating atoms $\gamma(t=0) \sim N$ to collectively enhanced emission $\sim N^2$.

In the Kuramoto model, synchronization is quantified by the order parameters

$$r e^{i\psi} = \frac{1}{N} \sum_{n=1}^N e^{i\phi_n}, \quad (52)$$

where $0 \leq r \leq 1$ is the coherence and ψ is the average phase. Individual trajectories of the Dicke decay in TWA, denoted by the subscript (j), indeed share the feature of emerging transient coherence as is shown in Fig. 2. Even though the coherences $r_{(j)}$ approach zero at short and long times, there is an intermediate window where they peak significantly. Around this peak, the change of the phases in time vanishes and the signal-to-noise ratio is strongly enhanced. At the same time, the slope of the number of excitations is minimal, i.e. a photon emission burst occurs.

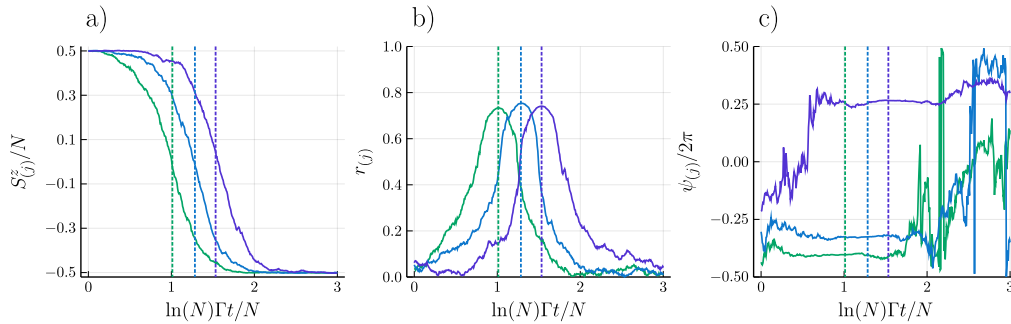


Figure 2: Time evolution of three sample trajectories according to the Dicke decay in TWA with $N = 256$ atoms. Depicted are a) the number of excitations, b) coherences and c) average phases of the atomic ensemble. The dashed vertical lines denote times of peak coherence.

At first glance this coherent locking of phases might be surprising when compared to the rate equation of the density operator which does not show such an effect. We note however that the emerging average phase $\psi_{(j)}$ of a single trajectory during the burst is uniformly distributed. By taking an additional trajectory average *before* computing the order parameters, the coherence vanishes at all times.

6 Dynamics of Spatially Extended Systems

Let us now turn to the more realistic spatially extended systems, where idealizations such as the Dicke model are no longer sufficient. We first consider a dense elongated cloud of trapped atoms with a size comparable or slightly larger than the transition wavelength, which corresponds to actual experimental realizations of Dicke superradiance [3, 48]. As a second example we consider the recently developed light-matter interfaces based on regular arrays of atoms [49] with sub-wavelength lattice constants. In these arrays interference from the precisely positioned atomic emitters leads to pronounced collective responses despite a comparatively small number of atoms. Using atomic configurations inspired by these recent experimental advancements, we benchmark the performance of the TWA based on the truncated correspondence rules with numerically exact results.

The atomic ensembles are treated according to their full master equation of Eq. (38) including dissipation and the dipole-dipole interactions. The numerical predictions are obtained from solving the SDEs of Eqs. (43). For all examples we choose a timestep $\Gamma_0 \Delta t = 10^{-3}$ and $N_{\text{Traj}} = 64 \cdot 10^3$ trajectories for the TWA simulations. We compare the semiclassical predictions to Monte Carlo wavefunction (MCWF) simulations of small systems obtained by using the *QuantumOptics.jl* package [50]. These are, apart from stochastic fluctuations due to a finite number of trajectories, exact. All MCWF expectation values were calculated from $N_{\text{Traj}} = 10^3$ trajectories.

6.1 Superradiance from an extended atomic cloud driven by an external laser

Let us start by considering superradiance of an ensemble of $N = 50$ atoms in an extended, three-dimensional harmonic trap, see Fig. 3 a). The positions of the atoms are normally distributed with standard deviation ξ_μ along each dimension and vanishing mean. We choose $\xi_{x,y} = 0.15\lambda_e$ and $\xi_z = 5.5\lambda_e$ such that the cloud is cigar-shaped. Here and in the next sec-

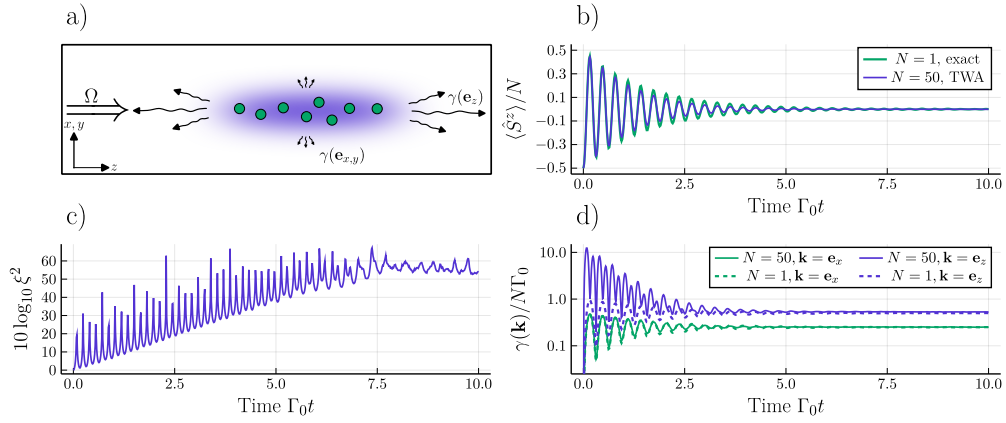


Figure 3: Comparison of the dynamics of a cigar-shaped cloud of 50 atoms and a single atom. a) Sketch of the geometry of the gas and incoming and outgoing light. b) Average excitation number as function of time. c) Spin squeezing of the cloud as predicted by the TWA. d) Directed photon emission rate into the x-direction (green lines) and z-direction (blue lines).

tions, each atom is assumed to have a dipole allowed transition from the ground state $|g\rangle$ to the excited state $|e\rangle$ with circular polarization $\mathbf{e}_p = (1, i, 0)^T / \sqrt{2}$. They are driven by a plane wave with $\mathbf{k}_c = \frac{2\pi}{\lambda_e} \mathbf{e}_z$ such that we obtain Rabi frequencies $\Omega_n = \Omega e^{i\mathbf{k}_c \cdot \mathbf{r}_n}$ with $\Omega = 20\Gamma_0$.

In Fig. 3 the dynamics of the cloud is compared to that of a single atom in free space. The incoming field drives damped Rabi oscillations whose magnitude is weakly suppressed due to collective effects. The photon emission rate $\gamma(\mathbf{e}_x)$ along the x-direction is not significantly changed by the presence of several atoms and coincides with the emission into the y-direction.

In stark contrast to this, the emission into the z-direction shows several strong superradiant bursts during the first few Rabi cycles. The steady state photon emission rate $\gamma(\mathbf{e}_{x,y})$ is enhanced by 0.6% relative to the single-particle case, whereas the emission along \mathbf{e}_z is increased by 6.3%.

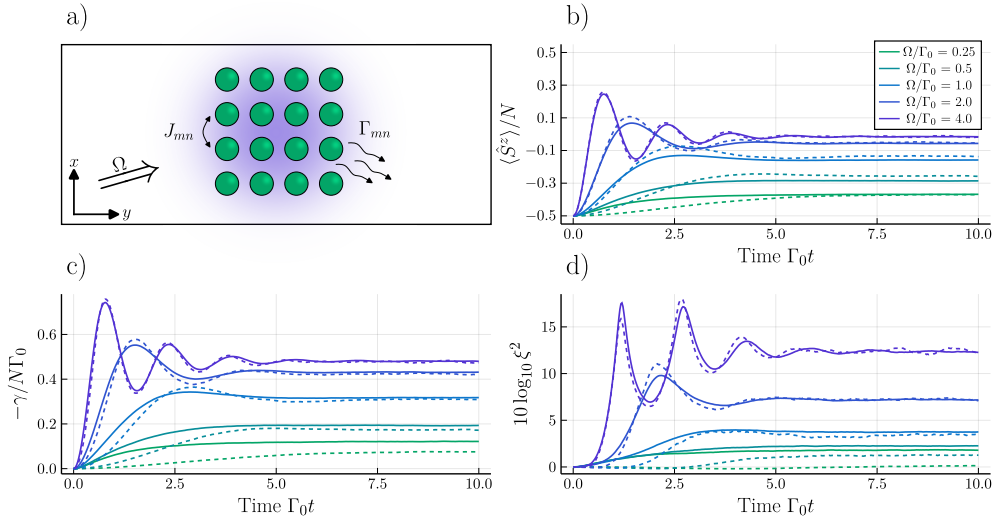


Figure 4: Dynamics of a coherently driven 4×4 quadratic atomic array with lattice spacing $a = 0.8\lambda_e$. a) Sketch of the array that is aligned in the x-y-plane and driven by a plane wave propagating along the z-axis. b) Total excitation number, c) total photon emission rate into free space and d) spin squeezing for a coherently driven atomic array as a function of time. The TWA predictions (solid lines) are compared to MCWF simulations (dashed lines). The different colors denote varying Rabi frequencies Ω .

6.2 Driven atomic arrays

Let us now consider an array of $N = 16$ atoms on a 4×4 quadratic lattice in the x-y-plane with lattice constant $a = 0.8\lambda_e$. We again drive the atoms with a plane wave propagating along the z-direction, i.e. perpendicular to the array, such that $\Omega_n = \Omega$. The atoms are initially in the collective ground state $|g_1 g_2 \dots g_N\rangle$.

In Fig. 4 we see that the interplay of driving and dissipation leads to damped Rabi oscillations in the number of excitations and finally to a non-trivial steady state. At small driving $\Omega/\Gamma_0 < 1$ the TWA does not reproduce the transient dynamics and steady state values obtained from MCWF simulations, which are still feasible for this small number of emitters.

As the driving increases, the match between semiclassical and exact dynamics improves. In the moderate to strong driving regime $\Omega/\Gamma_0 \geq 1$ we see a very good agreement across all observables. Most notably, the spin squeezing parameter is matched closely, suggesting an overall excellent prediction of general second moments.

The ever improving performance in the strong driving regime $\Omega/\Gamma_0 \geq 1$ can be explained by the competition of the driving and the dissipation. Here, only the cooperative, i.e. superradiant, modes significantly contribute to the dynamics. On the other hand, subradiant modes with their weak rates become insignificant for the overall dynamics and the steady state.

6.3 Inverted atomic arrays

Now we analyze the relaxation of an initially fully inverted state $|e_1 e_2 \dots e_N\rangle$ in the absence of a classical driving field, i.e. we set $\Omega_n = 0$. The atoms again form a 4×4 quadratic array in the x-y-plane with a smaller lattice constant of $a = 0.2\lambda_e$.

In Fig. 5 a) we see the comparison between the TWA prediction and a MCWF simulation. The dynamics can be split into two time regimes: The superradiant regime $\Gamma_0 t \lesssim 1$ and the subradiant regime $\Gamma_0 t \gtrsim 1$. The TWA closely matches the exact results during the superradiant

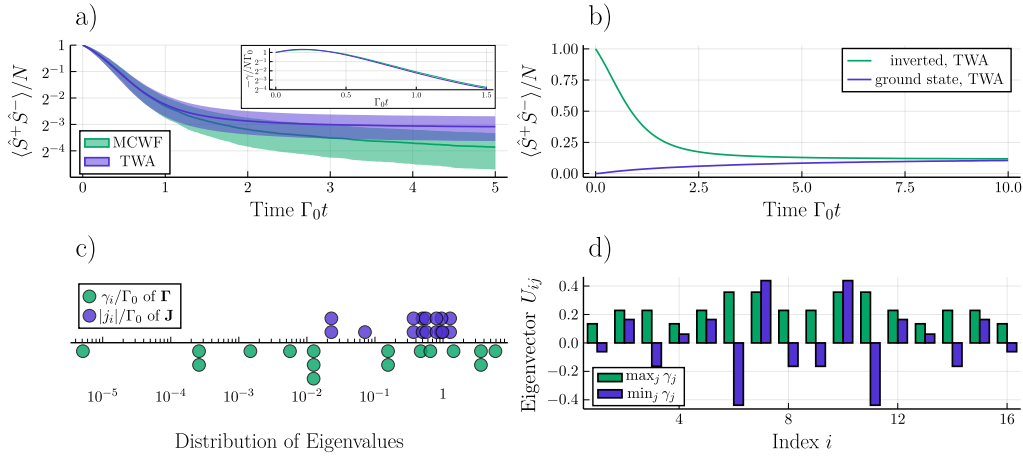


Figure 5: a) Number of excitations in the atomic array as a function of time as predicted by the TWA (blue) and by a MCWF simulation (green). The shaded areas denote half variances $\Delta S^z/2$ and the inset shows the total photon emission rate at early times. b) TWA prediction of the number of excitations starting from the fully inverted state (green line) and the collective ground state (blue line). c) Distribution of the eigenvalues γ_i of the dissipation matrix Γ and $|j_i|$ of the dipole-dipole interaction matrix J . Stacked points denote degeneracies. d) Weights of the most superradiant and subradiant eigenvectors of Γ .

burst. As the system transitions into subradiance, the semiclassical prediction converges to a finite number of excitations $\langle \hat{S}^+ \hat{S}^- \rangle \approx N/10$, i.e. it *gets stuck* at a subradiant plateau which is unstable in a full quantum treatment. We verify that this is a steady state according to the TWA by comparing it to a second semiclassical evolution starting from the collective ground state as shown in b) where, even in the absence of any excitation processes, the system evolves out of the collective ground state. Similar unphysical creation of excitations in systems with subradiant modes, though not as pronounced, has also been observed in cumulant expansion approaches [20, 21].

This can be explained by the distribution of the eigenvalues of Γ and J as can be seen in c). At the timescale $\Gamma_0 t \leq 1$ the rates γ_i of the cooperative superradiant eigenmodes of the matrix $\Gamma = U \cdot \text{diag}(\{\gamma_j\}) \cdot U^T$ dominate the dynamics, whereas the eigenvalues j_i of the dipole-dipole interaction matrix J only significantly contribute at $\Gamma_0 t \gtrsim 1$.

In d) we show the amplitude distribution of the most superradiant (green) and subradiant eigenvectors (blue) of U_{ij} . The superradiant mode is strongly cooperative as all coefficients have the same sign and are of approximately equal magnitude. In contrast, the subradiant mode has alternating signs and couples the atoms with more varying magnitudes. The validity criterion of Eq. (30) is satisfied when the superradiant mode acts on the collective ground state, but for the subradiant mode it is not. The presence of several modes with eigenvalues $10^{-2} < \gamma_i/\Gamma_0 < 10^0$ shows that such low-cooperativity effects already become relevant at the timescale of the simulation and therefore the TWA fails to escape the plateau.

7 Conclusion

We here presented a semiclassical, numerically efficient approach to describe the many-body dynamics of spins with collective interactions and dissipation. The approach is an extension of

the discrete truncated Wigner approximation [24], which approximates the time evolution of a physical state in the Wigner phase space by a diffusion-like process taking into account classical and leading-order quantum fluctuations. The equation of motion of the Wigner distribution of the many-body density matrix can be cast into a differential form by applying correspondence rules, i.e. the action of an operator on the state translated into phase space. We proposed a specific truncation of said correspondence rules by only keeping lowest-order contributions which maps the Lindblad master equation of interacting two-level systems to a Fokker-Planck equation with positive diffusion. The latter allows for a numerically inexpensive propagation in time by solving only linearly many stochastic differential equations.

We derived quantifiable conditions for the validity of the approximation in terms of an upper bound on the error that is introduced by the truncation. We showed in particular that the truncation becomes exact if the many-body dynamics is dominated by degrees of freedom with high cooperativity in a large ensemble. Thus the method is ideally suited for the analysis of collective processes such as superradiant emission of light in atomic ensembles. We benchmarked our method against exact results for the Dicke decay, which can be obtained without further approximations and found excellent agreement that improves with the number of atoms in the ensemble. Furthermore we study the dynamics of a driven, harmonically trapped, spatially extended ensemble of quantum emitters and calculated its population dynamics, spin squeezing and direction resolved photon emission rates. In the case of small atomic arrays, we compared predictions from our semiclassical approach with exact Monte Carlo wavefunction results and showed that early superradiant timescales are well captured, however longer subradiant timescales cannot be reliably described. When the array is coherently driven with Rabi frequencies at or above the single-particle linewidth, the influence of the subradiant modes becomes negligible and the emerging dynamics is again well captured within the semiclassical approximation.

Our approach paves the way for studying strongly cooperative effects in large and spatially extended ensembles of two-level systems. Specifically, recent light-matter interfaces such as trapped gases and atomic arrays and their non-linear response to incoming coherent light [48, 49] can be studied with ensemble sizes much larger than $N \simeq 50$ as is considered in this work. Typically, not much analytical progress can be made in such systems and methods based on tensor networks do not work reliably due to the high dimensionality of these setups and intrinsic long-range interactions.

Future works will investigate whether the truncation, which so far is a diffusion approximation, can be improved by extending it to a jump-diffusion approximation by including classical Poissonian jump processes. This might allow for an extension of the validity of our theory to regimes of moderate or even low cooperativity. Motivated by the excellent agreement of second moment expectation values such as spin squeezing, we believe that our method can be used to analyze the generation of non-classical states of realistic, experimentally realizable atomic configurations and their emitted light.

Funding information The authors gratefully acknowledge financial support by the DFG through SFB/TR 185, Project No. 277625399.

References

- [1] R. H. Dicke, *Coherence in spontaneous radiation processes*, Phys. Rev. **93**, 99 (1954), doi:[10.1103/PhysRev.93.99](https://doi.org/10.1103/PhysRev.93.99).
- [2] N. E. Rehler and J. H. Eberly, *Superradiance*, Physical Review A **3**(5), 1735 (1971).

- [3] M. Gross and S. Haroche, *Superradiance: An essay on the theory of collective spontaneous emission*, Physics Reports **93**(5), 301 (1982), doi:[https://doi.org/10.1016/0370-1573\(82\)90102-8](https://doi.org/10.1016/0370-1573(82)90102-8).
- [4] N. Skribanowitz, I. Herman, J. MacGillivray and M. Feld, *Observation of dicke superradiance in optically pumped hf gas*, Physical Review Letters **30**(8), 309 (1973).
- [5] M. Gross, C. Fabre, P. Pillet and S. Haroche, *Observation of near-infrared dicke superradiance on cascading transitions in atomic sodium*, Physical Review Letters **36**(17), 1035 (1976).
- [6] R. DeVoe and R. Brewer, *Observation of superradiant and subradiant spontaneous emission of two trapped ions*, Physical review letters **76**(12), 2049 (1996).
- [7] D. Chang, J. Douglas, A. González-Tudela, C.-L. Hung and H. Kimble, *Colloquium: Quantum matter built from nanoscopic lattices of atoms and photons*, Reviews of Modern Physics **90**(3), 031002 (2018).
- [8] M. Fleischhauer and M. D. Lukin, *Dark-state polaritons in electromagnetically induced transparency*, Physical review letters **84**(22), 5094 (2000).
- [9] A. Kozhekin, K. Mølmer and E. Polzik, *Quantum memory for light*, Physical Review A **62**(3), 033809 (2000).
- [10] A. Asenjo-Garcia, M. Moreno-Cardoner, A. Albrecht, H. Kimble and D. E. Chang, *Exponential improvement in photon storage fidelities using subradiance and “selective radiance” in atomic arrays*, Physical Review X **7**(3), 031024 (2017).
- [11] L.-M. Duan, M. D. Lukin, J. I. Cirac and P. Zoller, *Long-distance quantum communication with atomic ensembles and linear optics*, Nature **414**(6862), 413 (2001).
- [12] M. D. Lukin, M. Fleischhauer, R. Cote, L. Duan, D. Jaksch, J. I. Cirac and P. Zoller, *Dipole blockade and quantum information processing in mesoscopic atomic ensembles*, Physical review letters **87**(3), 037901 (2001).
- [13] D. Maxwell, D. J. Szwer, D. Paredes-Barato, H. Busche, J. D. Pritchard, A. Gauguet, K. J. Weatherill, M. P. A. Jones and C. S. Adams, *Storage and control of optical photons using rydberg polaritons*, Phys. Rev. Lett. **110**, 103001 (2013), doi:[10.1103/PhysRevLett.110.103001](https://doi.org/10.1103/PhysRevLett.110.103001).
- [14] T. Peyronel, O. Firstenberg, Q.-Y. Liang, S. Hofferberth, A. V. Gorshkov, T. Pohl, M. D. Lukin and V. Vuletić, *Quantum nonlinear optics with single photons enabled by strongly interacting atoms*, Nature **488**(7409), 57 (2012).
- [15] D. E. Chang, V. Vuletić and M. D. Lukin, *Quantum nonlinear optics—photon by photon*, Nature Photonics **8**(9), 685 (2014).
- [16] K. Mølmer, Y. Castin and J. Dalibard, *Monte carlo wave-function method in quantum optics*, JOSA B **10**(3), 524 (1993).
- [17] U. Schollwöck, *The density-matrix renormalization group in the age of matrix product states*, Annals of physics **326**(1), 96 (2011).
- [18] S. Masson and A. Asenjo-Garcia, *Universality of dicke superradiance in arrays of quantum emitters*, Nature Communications **13** (2022), doi:[10.1038/s41467-022-29805-4](https://doi.org/10.1038/s41467-022-29805-4).

- [19] F. Robicheaux, *Theoretical study of early-time superradiance for atom clouds and arrays*, Phys. Rev. A **104**, 063706 (2021), doi:[10.1103/PhysRevA.104.063706](https://doi.org/10.1103/PhysRevA.104.063706).
- [20] F. Robicheaux and D. A. Suresh, *Beyond lowest order mean-field theory for light interacting with atom arrays*, Phys. Rev. A **104**, 023702 (2021), doi:[10.1103/PhysRevA.104.023702](https://doi.org/10.1103/PhysRevA.104.023702).
- [21] O. Rubies-Bigorda, S. Ostermann and S. F. Yelin, *Characterizing superradiant dynamics in atomic arrays via a cumulant expansion approach*, Phys. Rev. Res. **5**, 013091 (2023), doi:[10.1103/PhysRevResearch.5.013091](https://doi.org/10.1103/PhysRevResearch.5.013091).
- [22] K. J. Kusmieriek, S. Mahmoodian, M. Cordier, J. Hinney, A. Rauschenbeutel, M. Schemmer, P. Schneeweiss, J. Volz and K. Hammerer, *Higher-order mean-field theory of chiral waveguide qed* (2022), [2207.10439](https://arxiv.org/abs/2207.10439).
- [23] H. Ma, O. Rubies-Bigorda and S. F. Yelin, *Superradiance and subradiance in a gas of two-level atoms* (2022), [2205.15255](https://arxiv.org/abs/2205.15255).
- [24] J. Schachenmayer, A. Pikovski and A. M. Rey, *Many-body quantum spin dynamics with monte carlo trajectories on a discrete phase space*, Phys. Rev. X **5**, 011022 (2015).
- [25] C. D. Mink, D. Petrosyan and M. Fleischhauer, *Hybrid discrete-continuous truncated wigner approximation for driven, dissipative spin systems*, Physical Review Research **4**(4), 043136 (2022).
- [26] J. Huber, A. M. Rey and P. Rabl, *Realistic simulations of spin squeezing and cooperative coupling effects in large ensembles of interacting two-level systems*, Phys. Rev. A **105**, 013716 (2022).
- [27] V. P. Singh and H. Weimer, *Driven-dissipative criticality within the discrete truncated wigner approximation*, Phys. Rev. Lett. **128**, 200602 (2022), doi:[10.1103/PhysRevLett.128.200602](https://doi.org/10.1103/PhysRevLett.128.200602).
- [28] D. Walls and G. Milburn, *Quantum Optics*, Springer Study Edition. Springer Berlin Heidelberg (2012).
- [29] M. J. Steel, M. K. Olsen, L. I. Plimak, P. D. Drummond, S. M. Tan, M. J. Collett, D. F. Walls and R. Graham, *Dynamical quantum noise in trapped bose-einstein condensates*, Phys. Rev. A **58**, 4824 (1998).
- [30] A. Sinatra, C. Lobo and Y. Castin, *The truncated Wigner method for Bose-condensed gases: limits of validity and applications*, Journal of Physics B Atomic Molecular Physics **35**(17), 3599 (2002).
- [31] C. Gardiner, P. Zoller and P. Zoller, *Quantum noise: a handbook of Markovian and non-Markovian quantum stochastic methods with applications to quantum optics*, Springer Science & Business Media (2004).
- [32] A. Polkovnikov, *Phase space representation of quantum dynamics*, Ann. of Physics **325**, 1790 (2010).
- [33] C. Brif and A. Mann, *Phase-space formulation of quantum mechanics and quantum-state reconstruction for physical systems with lie-group symmetries*, Phys. Rev. A **59**, 971 (1999), doi:[10.1103/PhysRevA.59.971](https://doi.org/10.1103/PhysRevA.59.971).
- [34] A. B. Klimov, J. L. Romero and H. de Guise, *Generalized $su(2)$ covariant wigner functions and some of their applications*, Journal of Physics A: Mathematical and Theoretical **50**(32), 323001 (2017), doi:[10.1088/1751-8121/50/32/323001](https://doi.org/10.1088/1751-8121/50/32/323001).

- [35] D. Zueco and I. Calvo, *Bopp operators and phase-space spin dynamics: application to rotational quantum brownian motion*, Journal of Physics A: Mathematical and Theoretical **40**, 4635 (2006).
- [36] W. K. Wootters, *A wigner-function formulation of finite-state quantum mechanics*, Annals of Physics **176**(1), 1 (1987).
- [37] A. B. Klimov and P. Espinoza, *Moyal-like form of the star product for generalized $su(2)$ stratonovich-weyl symbols*, Journal of Physics A: Mathematical and General **35**(40), 8435 (2002), doi:[10.1088/0305-4470/35/40/305](https://doi.org/10.1088/0305-4470/35/40/305).
- [38] H. Carmichael, *An Open Systems Approach to Quantum Optics: Lectures Presented at the Université Libre de Bruxelles, October 28 to November 4, 1991*, Lecture Notes in Physics Monographs. Springer Berlin Heidelberg, ISBN 9783540476207 (2009).
- [39] C. Gardiner, *Stochastic Methods: A Handbook for the Natural and Social Sciences*, Springer Series in Synergetics. Springer Berlin Heidelberg (2010).
- [40] H. Risken and T. Frank, *The Fokker-Planck Equation: Methods of Solution and Applications*, Springer Series in Synergetics. Springer Berlin Heidelberg (1996).
- [41] R. Graham, *Covariant stochastic calculus in the sense of itô*, Physics Letters A **109**, 209 (1985).
- [42] C. Rackauckas and Q. Nie, *Differentialequations.jl—a performant and feature-rich ecosystem for solving differential equations in julia*, Journal of Open Research Software **5**(1), 15 (2017).
- [43] J. Huber, P. Kirton and P. Rabl, *Phase-space methods for simulating the dissipative many-body dynamics of collective spin systems*, SciPost Physics **10**(2), 045 (2021).
- [44] V. P. Singh and H. Weimer, *Driven-dissipative criticality within the discrete truncated wigner approximation*, Phys. Rev. Lett. **128**, 200602 (2022).
- [45] L. Allen and J. Eberly, *Optical Resonance and Two-Level Atoms*, Dover Books on Physics. Dover Publications, ISBN 9780486136172 (2012).
- [46] J. Ma, X. Wang, C. Sun and F. Nori, *Quantum spin squeezing*, Physics Reports **509**(2), 89 (2011), doi:<https://doi.org/10.1016/j.physrep.2011.08.003>.
- [47] J. A. Acebrón, L. L. Bonilla, C. J. Pérez Vicente, F. Ritort and R. Spigler, *The kuramoto model: A simple paradigm for synchronization phenomena*, Rev. Mod. Phys. **77**, 137 (2005), doi:[10.1103/RevModPhys.77.137](https://doi.org/10.1103/RevModPhys.77.137).
- [48] G. Ferioli, A. Glicenstein, I. Ferrier-Barbut and A. Browaeys, *Observation of a non-equilibrium superradiant phase transition in free space* (2022), [2207.10361](https://arxiv.org/abs/2207.10361).
- [49] J. Rui, D. Wei, A. Rubio-Abadal, S. Hollerith, J. Zeiher, D. Stamper-Kurn, C. Gross and I. Bloch, *A subradiant optical mirror formed by a single structured atomic layer*, Nature **583**, 369 (2020), doi:[10.1038/s41586-020-2463-x](https://doi.org/10.1038/s41586-020-2463-x).
- [50] S. Krämer, D. Plankensteiner, L. Ostermann and H. Ritsch, *Quantumoptics.jl: A julia framework for simulating open quantum systems*, Computer Physics Communications **227**, 109 (2018).